Energy dissipation during stationary flow of suspensions of hydrophilic and hydrophobic glass spheres in organic liquids

Energy Dissipation during Stationary Flow of Suspensions of Hydrophilic and Hydrophobic Glass Spheres in Organic Liquids[1]

A. J. G. VAN DIEMEN AND H. N. STEIN

Laboratory of Colloid Science, Vakgroep Elektrochemie, Department of Chemical Technology, Eindhoven University of Technology, Eindhoven, The Netherlands

Received February 20, 1981; accepted August 21, 1981

Suspensions of both hydrophilic and hydrophobic glass spheres in dioctylphthalate behave similarly to suspensions of hydrophilic glass spheres in glycerol + water mixtures: Newtonian behavior is shown up to a solid volume fraction (c_v) of 0.4; at larger c_v values, Bingham behavior is observed with a yield value steeply increasing at $c_v > 0.45$. Suspensions of hydrophobic glass spheres in glycerol + water mixtures, on the other hand, already show deviations from Newtonian behavior at $c_v < 0.1$. The phenomena indicate absence of coagulation in dioctylphthalate. The number of collisions between the glass spheres in noncoagulating suspensions with $0.45 < c_v < 0.58$ is calculated. That part of the energy dissipated per collision, which is independent of the mutual velocity of the colliding particles, cannot be accounted for by the attractive potential energy between the spheres as calculated by the Hamaker equation; in this respect the situation is analogous to that observed on floc formation in coagulating suspensions. It is suggested that the energy dissipation concerned is caused by the motion of spheres in the vicinity of a colliding pair, with the number of spheres entrained decreasing with increasing mutual velocity of the colliding spheres.

INTRODUCTION

Rheological properties of suspensions during stationary flow are interesting from a colloid chemical point of view because they are connected with the interaction between the suspended particles. This connection can be derived by considering the energy dissipation during flow per unit of volume and time macroscopically on the one hand; and on the other hand as a result of the interaction between the suspended particles, and between the particles and the surrounding medium.

Macroscopically considered, the energy dissipated in stationary flow per unit of volume and time is equal to $\tau \times D$ (τ = shearing stress, D = velocity gradient), independent of whether the flow is Newtonian or not.

In stationary flow, this work is completely dissipated and conducted away to the surroundings as heat. If we want to connect this energy dissipation with the interaction between the suspended particles, we must develop a model describing the number of encounters between the suspended particles. According to the simplest model, dating back to von Smoluchowski (1), the number of particles coming per unit of time within the "collision radius" R_{ij} of one particular particle is given by

$$p = (4/3)N_0 D R_{ij}^3 \qquad [1]$$

(N_0 = number of particles per unit volume, D = velocity gradient). The number of encounters per unit of time and volume then becomes

$$(1/2)pN_0 = (2/3)N_0^2 D R_{ij}^3. \qquad [2]$$

In the context of the present paper, it is im-

[1] Presented at the 4th International Conference on Surface and Colloid Science, Jerusalem, 5–10 July 1981.

0021-9797/82/040318-19$02.00/0

portant primarily that this number is proportional to D as long as R_{ij} is independent of D.

The energy dissipated during such an encounter may be supposed to be either due to transfer of momentum between passing particles, or to pair formation and separation (in stationary flow, as many pairs are separated as formed). In the former case, the energy dissipated per encounter will be proportional to the mutual velocity of the particles, hence proportional to D. In the latter case, it will be independent of it. Thus, the energy dissipation per unit of time and volume, as far as it is caused by the interaction between suspended particles, can be written as $AD^2 + BD$. In addition, there will be energy dissipation by momentum transfer between flow units of the suspending medium (E_L), and between the particles and the medium without interaction between the particles (E_{SL}). Thus

$$\tau D = E_L + E_{SL} + AD^2 + BD. \quad [3]$$

At low concentrations of solid particles, we obtain Newtonian behavior of the suspension; thus E_L and E_{SL} must both be proportional to D^2. However, the last term on the right-hand side in (3) is different; it will give rise to a Bingham yield value τ_0 which thus might give us indications on the energy dissipated on pair formation and separation. If no other particles are involved in the encounter between two particles, this energy is the depth of either the primary or the secondary minimum in the potential energy vs distance curve (2).

On closer inspection, the model is not quite appropriate. For one thing, R_{ij} is not independent of D as far as the number of encounters leading to pair formation is concerned. Thus, van de Ven and Mason (3), considering pair formation between equal spheres of radius r, used $2r$ for R_{ij} in relation (1) but inserted in this relation a factor α_0 (the "capture efficiency"). They obtained for the number of collisions leading to pair formation, experienced by one particular particle:

$$p = (32/3)\alpha_0 N_0 D r^3, \quad [4]$$

where α_0 is slightly dependent on D (proportional to $D^{-0.18}$) if there is no repulsion. Furthermore, Firth and Hunter (4–6) reported that in coagulated suspensions the energy of pair formation and separation can account for only a negligible fraction of the energy dissipation $\tau_0 D$. Van de Ven and Hunter (7) could account for this energy dissipation through fluid movement inside flocs during collisions. Such fluid motion, however, is not independent of the mutual velocity of the flocs during collisions; it would lead to an energy dissipation during a collision which would be proportional to D and thus would give rise to an energy dissipation per unit of volume and time proportional to D^2, if the floc size is independent of D. However, Hunter and Frayne (8) report that the floc radius is a proportional to $D^{-0.41}$ such as to make $\alpha_0 D a^2$ independent of D; this leads to an energy dissipation per unit of volume and time proportional to D.

This result, obtained in coagulated suspensions, gives the impression of being a bit fortuitous. In view of this, it appeared to us to be interesting to investigate in what circumstances the flow of suspensions with little tendency to coagulation can be described as Bingham behavior, and whether here the formation and separation of pairs might account for the energy dissipation $\tau_0 D$.

In such suspensions, deviations from Newtonian behavior are observed only at rather large c_v values (>0.4) (c_v = volume fraction of solid), where it is not realistic to use a model involving the formation of flocs of finite dimensions which might depend on D. Since it appeared desirable to change the chemical character of the surface of the suspended particles, we investigated suspensions of glass spheres which can easily be made hydrophobic (9, 10).

EXPERIMENTAL

a. Materials

Dioctyl phthalate (DOP). Di-2-ethylhexyl phthalate, *ex* Hoechst (through Lamers & Indemans, 's-Hertogenbosch) of technical purity; viscosity (293°K): 0.793 P.

For preparing suspensions, samples were used which had been dried in a desiccator containing P_2O_5; but no difference in rheological behavior of either DOP or of suspensions prepared with it were found, using DOP "as received" or dried.

Glycerol + water mixtures. "Glycerol" *ex* Merck, pro analysi; viscosity (293°K) = 1.505 P; refractive index $n_D^{25} = 1.4533$. From the refractive index, the water content was estimated to be 13.07% m/m.

Glass spheres. ex Tamson (Zoetermeer); specific mass (293°K) 2750 $kg \cdot m^{-3}$. The sample was divided into fractions by dry sieving; from the fraction with diameter $\phi < 36$ μm, fractions with equivalent Stokes diameter between 10 and 15 μm were isolated by sedimentation in deionized water (without the addition of a peptizing agent). After isolation, these samples were dried at 393°K at atmospheric pressure. The size distributions of the various samples were determined by SEM (see Table I); they could be described with reasonable accuracy by average diameters $\bar{\phi}$ and standard deviations σ_ϕ. Figure 1 shows a typical SE micrograph, Fig. 2 a view at higher magnification of such untreated glass (called "hydrophilic"). The spherical character of the glass particles was ascertained by optical microscopy; in Figs. 1 and 2, which were taken under an angle of about 30°, the spheres appear distorted because of the large sample depth.

The particles were rendered hydrophobic as follows (9): 100 g of glass was added to a vigorously stirred mixture of 300 ml *n*-hexane (*ex* Merck, "reinst") and 3 ml dimethyl-dichlorosilane (*ex* B.D.H.). The stirring was continued for 2 hr; then the supernatant was decanted. The glass was washed five times with *n*-hexane (30 ml), and dried for three days at room temperature at a pressure of 30 Torr. This operation caused a shift in size distributions toward larger sizes, due to loss of small particles on decantation; thus sample 3 (Table I) when made hydrophobic became sample 4. Figure 3 shows a SE micrograph of a hydrophobic glass surface. Investigation of used samples showed that the hydrophobic layer on the glass was resistant to treatment with both DOP and glycerol + water mixtures.

b. Apparatus for Rheological Measurements

The viscosity of homogeneous liquids was measured in three Ubbelohde type viscom-

TABLE I

Size Distributions of Glass Samples Used

Sample number	Limits of volume fractions (μm) 20%	50% smaller than	80%	$\bar{\phi}$ (μm)	σ_ϕ (μm)	Character
1	10.26 μm	12.88 μm	15.14 μm	12.88	2.90	Hydrophilic
2	36.64	42.95	50.47	42.95	8.22	Hydrophilic
3	55.4	68.8	80.1	68.8	14.6	Hydrophilic
4	64.3	81.9	94.0	81.9	17.7	Hydrophobic
5	12.1	14.9	19.8	14.9	4.6	Hydrophilic
6	13.3	16.1	18.2	16.1	2.91	Hydrophobic
7	43.4	62.2	81.9	62.2	22.8	Hydrophilic

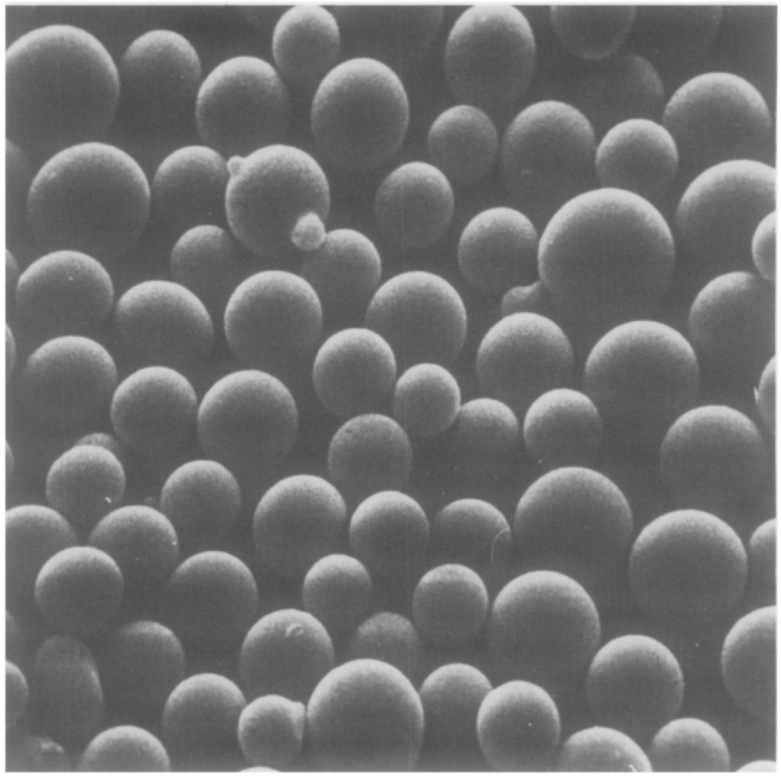

FIG. 1. SEM of glass sample 1. Horizontal side: 100 μm.

eters (inner diameters of the capillaries 2.8 $\times 10^{-3}$ m; length of the capillaries 8.5 $\times 10^{-2}$, 1.1 $\times 10^{-1}$ and 1.3 $\times 10^{-1}$ m, respectively).

Rheological measurements on both homogeneous liquids and on suspensions were performed in Epprecht rotational viscometers (Contraves A.G. Zürich). Two types were employed: Rheomat 15 and Rheomat 15T-FC; both had a stationary outer cylinder. The Rheomat 15T-FC permits the registration of time-dependent rheological properties. Two combinations of inner and outer cylinders were employed.

System	Radius of inner cylinder	Radius of outer cylinder	Effective length of inner cylinder
B	1.50×10^{-2}m	1.90×10^{-2}m	5.98×10^{-2}m
C	0.67×10^{-2}m	1.00×10^{-2}m	4.63×10^{-2}m

In order to minimize deviations of the movement of the inner cylinder from rotation about one axis, the rather loose coupling between the inner cylinder and the driving shaft in the apparatus as provided by Contraves A.G. was replaced by a brass body fixed to the driving shaft fitting closely about the shaft of the inner cylinder over a distance of 8 mm.

Angular velocities ranged from 0.586 to 36.9 rad $\cdot$ sec^{-1}; thus D ranged between 3.13 and 197.0 sec^{-1} for system B, and between 2.15 and 135.0 sec^{-1} for system C.

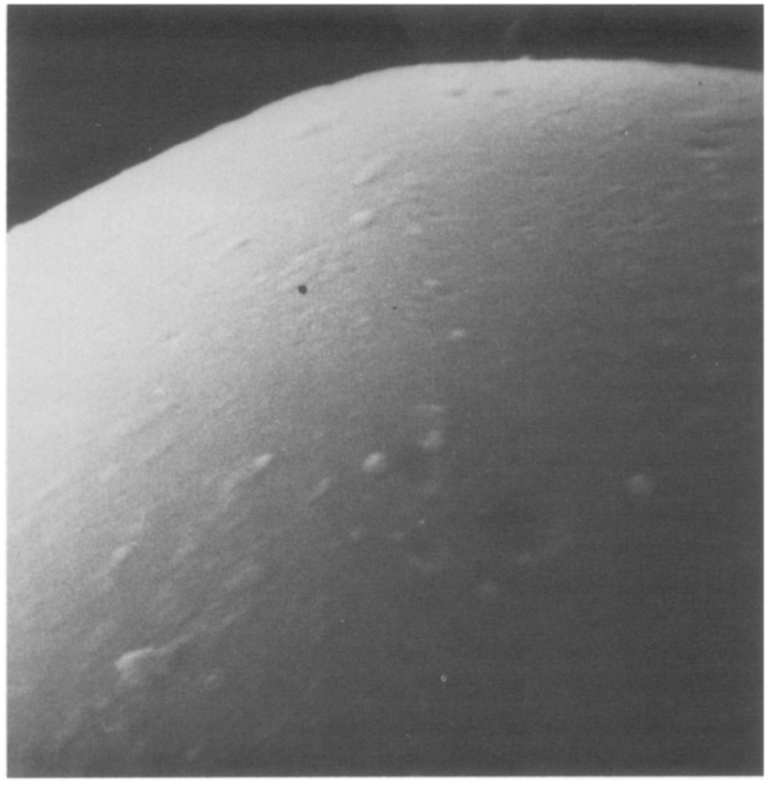

FIG. 2. SEM of glass sample 5 (hydrophilic). Horizontal side: 10 μm

The apparatus was calibrated with oils obtained from Fysisch Chemisch Instituut TNO (Zeist), showing Newtonian behavior with viscosities ranging from 4.41 to 9.67 P (293°K).

c. *Experimental Procedure*

Suspensions were prepared by mixing by hand. No detectable amounts of air (<0.1% by volume) became entrapped during the preparation of suspensions in DOP, and of suspensions of hydrophilic glass in glycerol + water mixtures; however, suspensions of hydrophobic glass in glycerol + water mixtures contained some air (≈3% at $c_v = 0.1$).

Rheological measurements were performed at 293.2 ± 0.1°K, by two methods:

1. "Time-dependence" method. At constant angular velocity, the torque was registered over 4 min after thorough homogenization of the suspension. Then the suspension was homogenized (by hand) and a measurement at another angular velocity was started. From the registered curves of the torque as a function of the time, values were read at 0.2, 0.4, 0.6, 0.8, 1, 2, 3, and 4 min after homogenization. In all cases, a steady-state result was obtained after about 2 min (one experiment was extended to 20 min without significant changes after the first 4 min). The torque values, read at one time after homogenization at different angular velocities, were combined into curves of the torque versus the angular velocities (see Figs. 6 and 9 for examples).

2. "Fast" method. In about 1 min, the angular velocity was raised from the lowest to the largest value and the sample was homogenized; then again in 1 min the angular velocity was decreased to the lowest

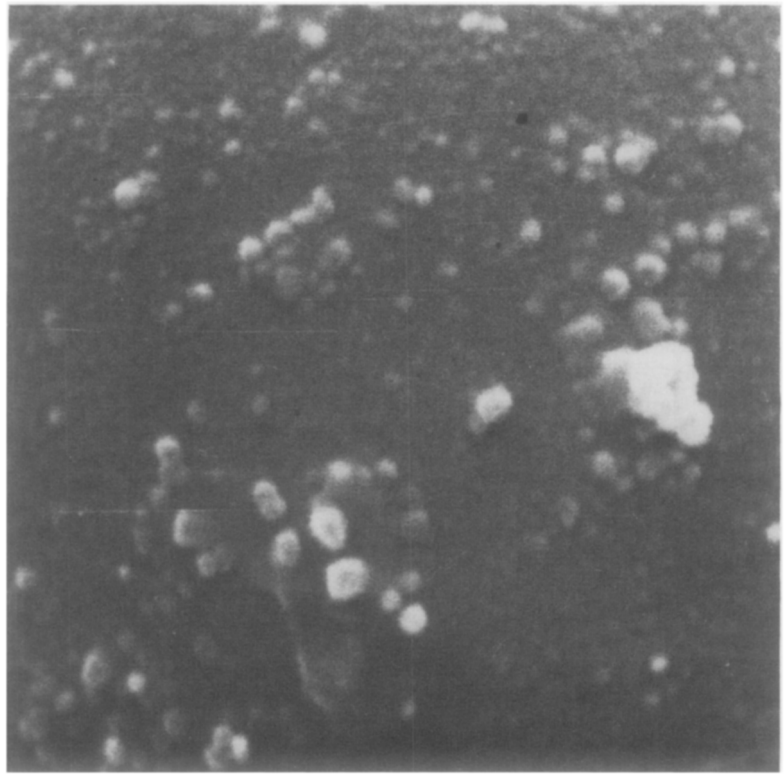

FIG. 3. SEM of glass sample 6 (hydrophobic). Vertical side: 10 μm.

value and the sample was homogenized. This was repeated. One run covered 5–7 angular velocities. Of the four values thus obtained for every angular velocity, an average was taken; no distinct hysteresis was found.

RESULTS

a. Suspensions in DOP

In DOP, most measurements were performed by the "fast" method since at low c_v values no deviations from time-independent Newtonian flow were observed; "time-dependence" measurements in DOP were restricted to $c_v = 0.50–0.549$, samples 3, 4, and 7.

Figure 4 shows the viscosities of various hydrophilic glass samples in DOP at $0 < c_v < 0.4$. These suspensions show a Newtonian behavior which is independent of the grain size, within the accuracy of the measurements. This fact implies that the measurements are not disturbed by a concentration gradient of the glass spheres caused by centrifugal force; centrifugal force separation would be 25 times more pronounced for sample 3 than for sample 1, and thus should lead to significantly lower viscosities at equal c_v values in sample 3 than in sample 1, if such a separation were of influence. At low c_v values, the viscosities approach the Einstein relation.

Figure 5 compares the rheological behavior of suspensions of hydrophobic and hydrophilic glass samples of similar size distributions. Again up to $c_v = 0.4$ Newtonian behavior is observed; at higher c_v values the rheological character can be described as Binghamian, both for "rapid"

and "time dependence" measurements (see, e.g., Fig. 6 for some typical results of "time dependence" measurements). In Fig. 5, for $c_v > 0.4$ the plastic viscosity ($=d\tau/dD$) is plotted. No significant influence is seen by the character (hydrophobic or hydrophilic) of the glass surface.

Figure 7 shows some values of the Bingham yield value τ_0 versus time observed by the "time-dependence" method. There exist no large discrepancies between the τ_0 and η values as found by the "rapid" method, and those found after 4 min by the "time-dependence" method.

Figure 8 shows τ_0 vs c_v as found by the "rapid" method for samples 3 and 4. τ_0 rises steeply at $c_v \geq 0.45$, again without any significant difference between hydrophilic or hydrophobic glass.

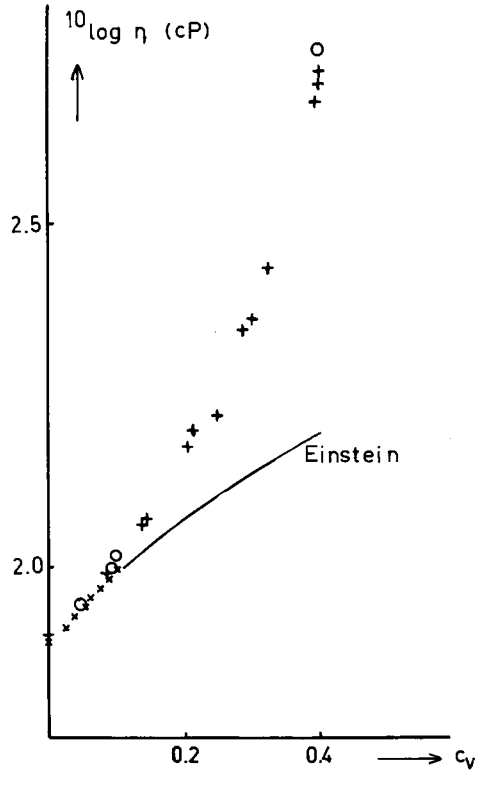

FIG. 4. Viscosity of suspensions of hydrophilic glass spheres in DOP. ×, sample 1; ○, sample 2; +, sample 3.

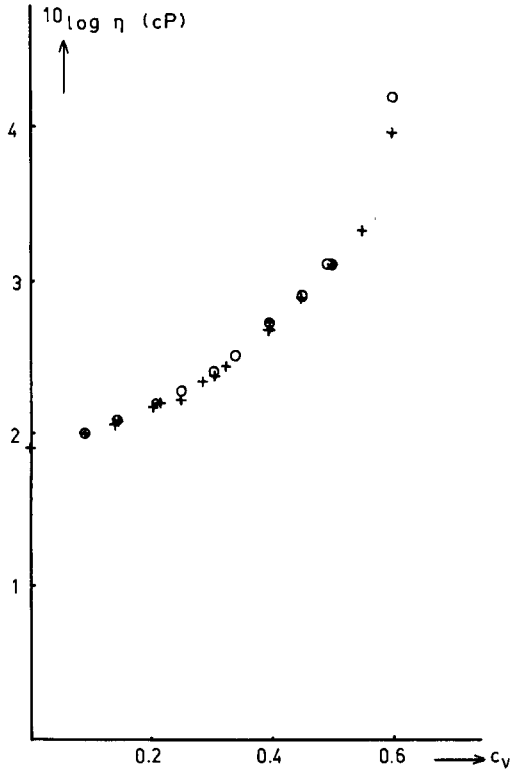

FIG. 5. Viscosities (c.q. plastic viscosities) of suspensions of hydrophilic and hydrophobic glass spheres in DOP. +, sample 3 (hydrophilic); ○, sample 4 (hydrophobic).

b. Suspensions in Glycerol + Water Mixtures

Suspensions in glycerol + water mixtures were investigated by the time-dependence and by the fast method, both in the concentration ranges $c_v \leq 0.4$ and $c_v \approx 0.5$.

Figure 9 shows typical experiments for a suspension of hydrophobic glass in glycerol + water mixtures, as observed by the "time-dependence" method: deviations from Newtonian behavior are observed, already at $c_v < 0.1$; but contrary to the data in DOP suspensions at large c_v values, no distinct time dependence is found in suspensions of hydrophobic glass in glycerol + water at $c_v < 0.2$. These suspensions coagulated rapidly; on the other hand, suspensions of hydrophilic glass in glycerol + water mixtures did not coagulate and

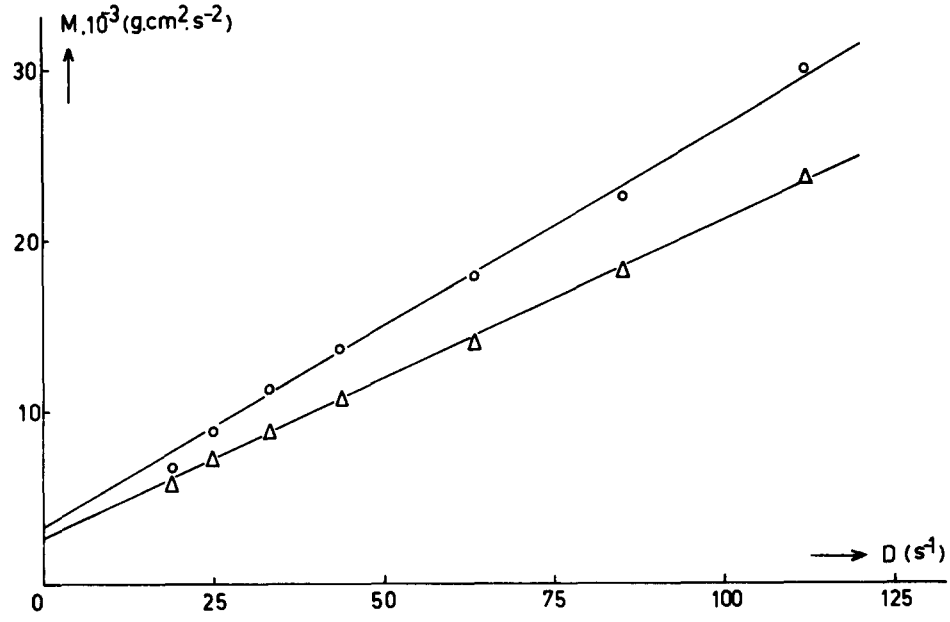

FIG. 6. Rheological data on a suspension of glass spheres (sample 7) in DOP, $c_v = 0.542$. "Time-dependence" method. M: torque exerted on inner cylinder. ○, after 0.2 min; △, after 4 min.

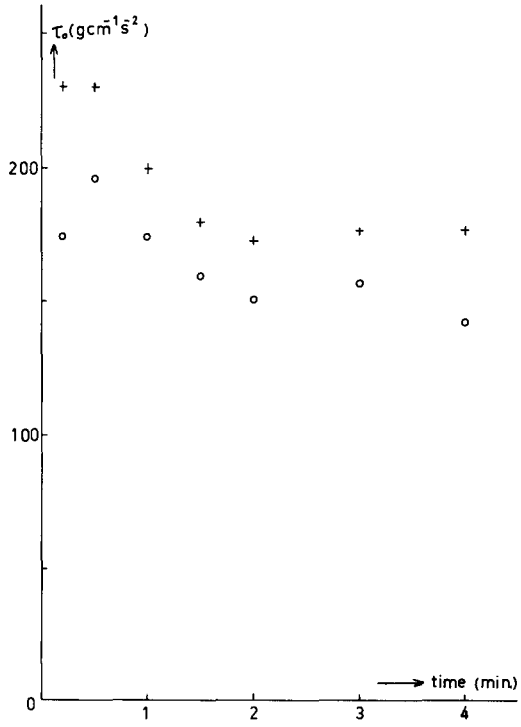

FIG. 7. τ_0 vs time in suspensions of glass spheres in DOP. +, sample 3, $c_v = 0.549$; ○, sample 7, $c_v = 0.542$.

showed Newtonian rheological behavior, at least for $c_v < 0.4$.

Figure 10 compares the viscosities of suspensions of hydrophilic and hydrophobic glass spheres, respectively, in glycerol + water mixtures. Here for suspensions of hydrophobic glass, the plastic viscosities are plotted. The plastic viscosity of suspensions of hydrophobic glass is seen to increase much more steeply with increasing c_v than the viscosity of suspensions of hydrophilic glass. τ_0 increases linearly with c_v^2 (Fig. 12), in accordance with the observations of Firth (5).

However, it should be noted that these suspensions contain some air (see earlier) which may influence the results.

DISCUSSION

It appears clearly from the experimental data that there is a distinct difference in behavior between suspensions in DOP, and in glycerol + water mixtures. In the latter, the character of the glass surface clearly

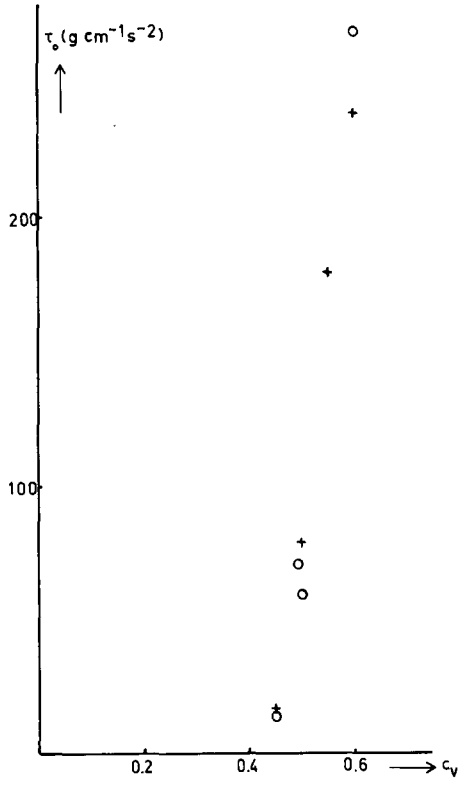

FIG. 8. τ_0 vs c_v in suspensions of glass spheres in DOP; "rapid" method. +, sample 3 (hydrophilic); ○, sample 4 (hydrophobic).

effects coagulation. A calculation of the interaction parameters according to Firth and Hunter (4–6) or Hunter and Frayne (8) was not attempted because it is rather problematic whether the assumptions of these authors apply to the systems concerned. Thus, on microscopic examination our suspensions of hydrophobic glass in glycerol + water mixtures were found to contain, in addition to agglomerates, quite a large number of single particles; furthermore, in the Hunter and Frayne analysis an important parameter, the "floc volume ratio" is calculated from the plastic viscosity by applying the Einstein relation, on the assumption that interactions between flocs influence only τ_0.

In DOP, on the other hand, no influence on the rheological behavior is found on making the glass surface hydrophobic. An explanation of this finding by postulating strong repulsion for both hydrophilic and hydrophobic spheres is not convincing: hydrophobic glass may be sterically stabilized in DOP by polymer chains protruding from the surface, but this cannot be invoked for hydrophilic surfaces. Electrostatic repulsion to the extent required for stabilizing the rather large glass spheres against coagulation is not very probable either. Thus, the absence of coagulation of both hydrophilic and hydrophobic glass spheres in DOP is explained most appropriately by the amphiphilic character of the DOP: the carboxyl groups in the DOP molecules attach themselves easily to hydrophilic glass surfaces, which leads to the protrusion of the hydrophobic chains into the DOP where there are enough other hydrophobic groups for strong interaction. Similarly, the hydrophobic glass surface can be visualized to be covered by the hydrophobic parts of the DOP molecules, with the polar groups protruding into the surrounding medium where they find enough similar groups for strong interaction. Nevertheless, it is remarkable that the absence of difference in rheological behavior of suspensions of hydrophilic and hydrophobic glass spheres extends to c_v values of 0.6.

In contrast with the situation in coagulating suspensions, τ_0 rises in noncoagulating suspension with $c_v > 0.4$ much more steeply than proportional with c_v^2 (compare Figs. 8 and 11). Thus in noncoagulating suspensions, the energy dissipation in stationary flow corresponding with $\tau_0 D$ cannot be correlated with collisions between either single particles of agglomerates as described by the von Smoluchowski theory of collisions between suspended flow units distributed at random.

A model describing the phenomena observed in noncoagulating suspensions must of course first of all be compatible with the occurrence of continuous flow up to $c_v \approx 0.6$. Thus, the hypothesis that three-dimensional

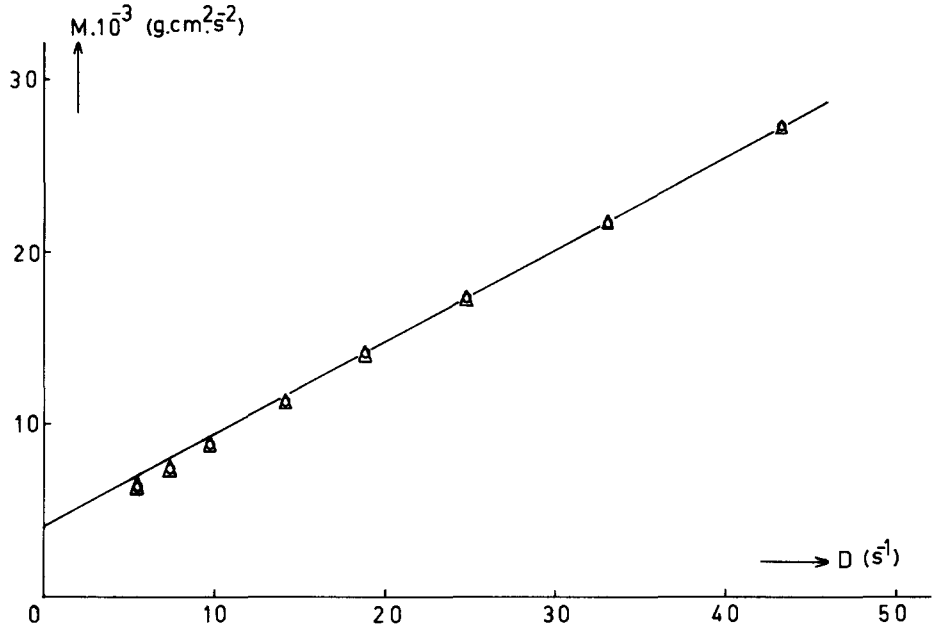

FIG. 9. Rheological data on a suspension of hydrophobic glass spheres (sample 6) in glycerol + water mixtures; c_v = 0.1735. "Time dependence" method. ○, 0.4 min; △, 4 min.

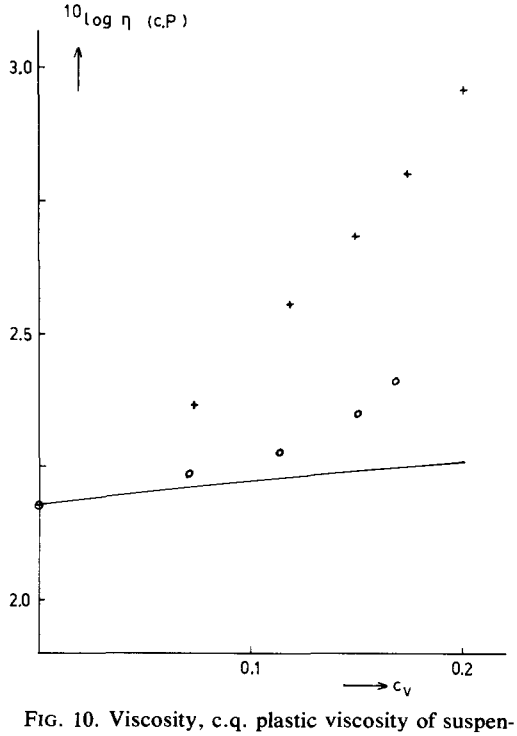

FIG. 10. Viscosity, c.q. plastic viscosity of suspensions of hydrophilic and hydrophobic glass spheres in glycerol + water mixture. ○, sample 5 (hydrophilic); +, sample 6 (hydrophobic).

domains are formed which move as independent units, which describes the phenomena in coagulated suspensions (4–6, 8), cannot account for the phenomena in noncoagulating suspensions, since it implies that a large part of the liquid is immobilized in these units; continuous flow is then difficult to visualize at high c_v. If we assume, for instance, within these units a c_v value of 0.72 (corresponding to hexagonal close packing of equal spheres), in a paste with an overall c_v = 0.6, the volume fraction of spheres and immobilized liquid becomes 0.83. The present authors see no possibility of continuous flow of independent units in these circumstances. If a system consisting of such three-dimensional units is subjected to a shearing stress, while flow of the units is not possible, the units themselves will break down; the more so because only weak bonds exist between the primary particles in noncoagulating suspensions.

Less liquid is immobilized, if the flow occurs through the gliding of layers over each other. When the mutual attraction be-

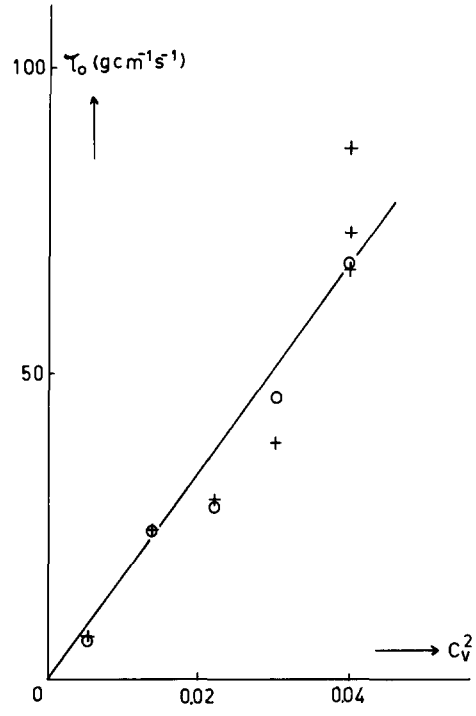

FIG. 11. τ_0 vs c_v^2 in suspensions of hydrophobic glass spheres (sample 6) in glycerol + water mixture. +, "rapid" method; ○, "time-dependence" method.

tween the suspended glass spheres is weak, and the hydrodynamic interaction is large, collisions between the spheres are avoided as long as possible. This tendency will, in suspensions of monodisperse spheres, arrange the particles into layers parallel to the direction of the motion, with adjacent layers gliding over each other. On the basis of this model, a number of collisions per unit of volume, time, and velocity gradient is predicted which is proportional to experimental τ_0 values in the region $0.45 < c_v < 0.58$.

Indeed, the formation of such layers has been observed by Hoffman (11, 12), where the spheres were arranged within the layers in hexagonal close packing. Though in our case deviations from monodispersity are more pronounced than in Hoffman's experiments, a hexagonal close packing within layers appears to be a reasonable hypothesis: a cubical arrangement of monodisperse spheres would lead to a blocking of flow near $c_v = 0.52$, where in reality τ_0 is relatively low. On the basis of this model, the time dependence of η and τ_0 (see Fig. 7) can be ascribed to the formation of these layers.

In Fig. 12a, two such layers are shown separated by a distance d. The liquid between the spheres in one layer (shaded in Fig. 12a) is thought to move in the main with the spheres; in order to realize a macroscopic velocity gradient D in the sample, the top layer in Fig. 12a must move with respect to the lower one with a velocity equal to $D = (2r + d)$, and there exists thus a velocity gradient $D = (2r + d)/d$ in the space between the layers.

In this idealized situation, there would be

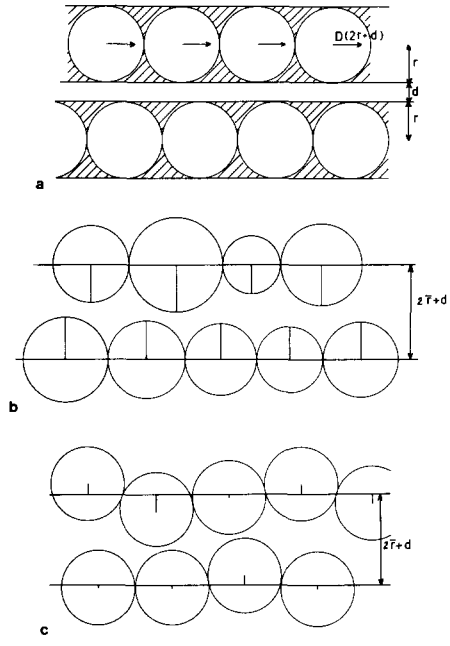

FIG. 12. Schematic representation of the model used for calculating the number of collisions in the flow of noncoagulating suspensions, $0.45 < c_v < 0.58$. (a) Idealized starting point: monodisperse spheres, no deviations from the layers. (b) First cause of deviations from the idealized starting point: not all spheres have the average radius $\bar{r}$, but they are still arranged in layers. (c) Second cause of deviations from the idealized starting point: the spheres are thought to be monodisperse, but the arrangement in layers is not perfect.

TABLE II

Values for K_1 and K_2 Calculated for Glass Sample 3, with A = 3.848×10^{-6} cm^2

c_v	K_1	K_2
0.49852	0.027294	0.02642
0.51923	0.051401	0.03980
0.53615	0.077981	0.05335
0.55719	0.118940	0.07339
0.57992	0.170861	0.09776

no collisions between the spheres at all. However, collisions may arise for two reasons:

1. if the spheres are not strictly monodisperse, deviation of their radius from the average may lead to collisions (Fig. 12b);

2. if the layers gliding over each other are not in fact ideally plane, deviation of the centers of the spheres from the centers of the layers may lead to collisions (Fig. 12c).

If K_1 is the chance that the passage of two spheres, with their centers in the centers of their respective layers, but with radii deviating from the average, is accompanied by a collision, and if K_2 is the chance that the passage of two spheres, both with "average" radius but with centers deviating from the centers of their respective layers, is accompanied by a collision, then the overall chance that a collision occurs on passage of two spheres can be approximated by

$$K_3 = K_1 + K_2 - K_1K_2. \qquad [5]$$

The last term in (5) accounts for the fact that there will be a number of collisions predicted by cause (b) which has already been predicted by cause (a).

Both K_1 and K_2 can be calculated numerically (see Appendixes 1 and 2, respectively; some results for typical experimental conditions are shown in Table II). It will be seen that these calculations start from a rectilinear approach of two colliding spheres; this appears, in view of the fact that the spheres are supposed to be forced toward a collision by their surroundings, to be more realistic in our case than the curvilinear approach forming the basis of Van de Ven and Mason's analysis (3). The latter is more appropriate if the spheres are moving freely in the surrounding liquid; for this to be operative, however, the c_v values are too large in the case at hand. In addition, it will be seen that both the forces arraying the spheres into layers, and the forces disarranging the layers, are supposed to find their origin in the viscous flow in the space between the layers. This is reasonable, as long as the motion of a sphere, caused by a collision, is damped sufficiently before the next collision. This effect is estimated by comparing the time necessary to reduce the velocity of a freely moving sphere to 1/2 of its initial value by viscous friction, with the time elapsing between two successive collisions. The former is 6×10^{-6} sec for a sphere of radius 35 μm and density 2.75 kg·m^{-3} in a liquid of $\eta = 0.793$ P; the latter is, at the largest velocity gradients employed in the present investigation, about 10^{-2} sec (the time between two passages of spheres in adjacent layers is about 2×10^{-3} sec, but not every passage will lead to a collision). From these values, it appears that viscous effects predominate in the arranging of the suspended particles.

Nevertheless, it is felt that the hypothesis that both the arraying of spheres into layers and the disarranging of these layers originate from the viscous flow in the space between the layers, limits the applicability of the model at the high c_v side, viz., near the c_v value where, with a hexagonal close packing of monodisperse spheres in layers, there would be no interlayer liquid ($d = 0$; $c_v \approx 0.6$).

The number of collisions per unit of volume and time will then be given by

$$(1/2) \times \text{number of spheres per unit of volume} \times \text{number of passages executed by one sphere per unit of time} \times K_3 = \frac{1}{2} \times \frac{c_v}{(4/3)\pi\bar{r}^3} \times D \times \frac{2\bar{r} + d}{\bar{r}} \times K_3. \qquad [6]$$

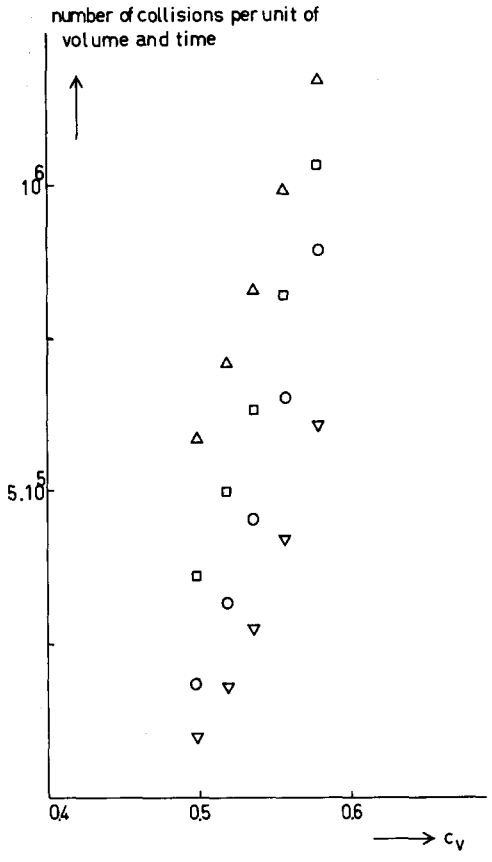

FIG. 13. Number of collisions per unit of volume and time, calculated from the model. $\bar{r} = 34.4$ μm, $\sigma = 7.31$ μm. $\nabla, A = 0$; $\circ, A = 3.848 \times 10^{-6}$ cm^2; $\square, A = 1.283 \times 10^{-5}$ cm^2; $\triangle, A = 3.848 \times 10^{-5}$ cm^2.

Some calculations, referring to glass sample 3 (see Table I) employed in part of the experiments described in Fig. 8, are shown in Fig. 13. In Fig. 14, τ_0 is plotted vs c_v on the same scale as used in Fig. 13; here some experiments are included which could not be represented well in Fig. 8. The rapid rise of τ_0 in the range between $c_v = 0.4$ and 0.6 is seen to be matched well by the rise in the number of collisions per unit of volume time and velocity gradient predicted by the model, especially if A is about 2×10^{-5} cm^2 which means that about 50% of the viscous flow energy dissipation in the interlayer liquid is used for disarranging the layers (see Appendix 2).

Passing over to a sample with about equal $\bar{r}$ but different σ will cause a larger number of collisions on the one hand, but a shift of the curve in Fig. 13 to the right on the other hand, because the solid volume fraction within the layers may then surpass the value corresponding with a hexagonal close packed arrangement of equal spheres, which forms the basis of the c_v assignment in Fig. 13. Since these effects counteract each other, no large influence of increasing heterodispersity on the number of collisions at a given c_v value is expected, which agrees with the experimental data (Fig. 14). With very heterodisperse suspensions the model loses its applicability.

Nevertheless, the energy dissipated per collision calculated by comparing the model with the experimental data, cannot be accounted for by the mutual attraction of the spheres as predicted by the Hamaker equation (13). Let us take, for instance, the data at $c_v = 0.52$. The number of collisions per

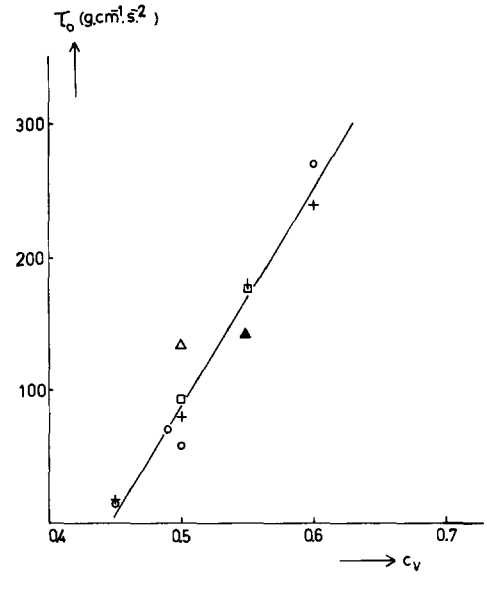

FIG. 14. τ_0 vs c_v in the range $0.4 < c_v < 0.6$. Experiments in suspensions in DOP. +, sample 3, "rapid" method; ○, sample 4, "rapid" method; □, sample 3, "time-dependence" method; △, sample 6, "time-dependence" method; ▲, sample 7, "time-dependence" method.

unit of volume (cm^3) time (sec) and velocity gradient (sec^{-1}) will be about 6×10^5 cm^{-3} for glass sample 3 (see Fig. 13). At this c_v value, τ_0 is about 120 $g \cdot cm^{-1}$ sec^{-2} (see Fig. 14), which gives an energy of 2×10^{-4} g cm^2 sec^{-2} dissipated on one collision. If this is ascribed wholly to the energy released on pair formation as described by the Hamaker equation, it should be equal to $-A_{12} \times r/(12 \times H)$, where A_{12} = the Hamaker constant and H = the distance of closest approach between colliding spheres. For A_{12} we take 2.5×10^{-12} erg (the value for TiO_2 in *p*-xylene (14)), thought to represent an upper limit in view of the absence of coagulation of glass spheres in DOP. This would lead, however, to an impossible value (3×10^{-12} cm) for H; smaller values of A_{12} would lead to still smaller values of H.

Some possible causes of this discrepancy, which have been discarded on second thoughts, are:

a. deviations of the glass particles from the ideal spherical form might effect an approach to a distance of, say, 0.3 nm over a larger area: calculations on the basis of flat plate interaction show that the particles should be able, if this effect is the cause of the discrepancy, to approach each other to 0.3 nm over an area of 2.7×10^{-6} cm^2 which is at variance with the EM data (Fig. 1);

b. interaction at close approach might be described by stronger attraction than is accounted for by the Hamaker equation (e.g., the interaction might be connected with chemical bond formation); this idea is not supported by the absence of differences between suspensions of hydrophilic and hydrophobic glass in DOP, even at large c_v values;

c. the model employed might predict a too low number of collisions per unit of volume and time; in order to bridge the gap between τ_0 and the theoretical value for the energy released on pair formation, at least 1000 times as much collisions are required as calculated from the model presented, and we do not see a reasonable way to achieve this.

The situation is completely analogous to that observed for coagulated suspensions where by a similar reasoning Hunter and colleagues also arrived at unacceptable values for H (4, 15). The most appropriate explanation in our case might be similar to that offered by Firth and Hunter (6): the energy dissipation on a collision occurs mainly through the motion of spheres in the vicinity of a colliding and separating pair. It is true that this motion should be proportional to the velocity gradient in the sample (7) and thus can only account for an energy dissipation per unit of volume and time, which itself is $\sim D$ if the number of entrained neighbors decreases with increasing D. The possibility that the size of the agglomerates decreases with increasing D, which is the obvious conclusion in the case of coagulated suspensions of low c_v (8), is not applicable in our case of suspensions with large c_v values. However, it could be that during a rapid collision, fewer neighboring spheres are entrained than during a slow one: during a rapid encounter, a large fraction of the local stress is caught elastically, whereas during a slow encounter the local stress sooner causes viscous motion of adjacent spheres.

The fraction of the local stress caught elastically might be returned to the flow field by the following (tentative) mechanism:

An elastic disarrangement caused by a collision with a sphere in a neighboring layer will generally have a component perpendicular to the layer. Thus a particle protruding from the top of its layer and colliding with a particle in the neighboring layer at the top, will in general move toward the bottom of its layer. It then becomes surrounded by liquid moving in the same directions as it moves itself on readjustment of its elastic displacement. Thus, less energy is dissipated than would be the case if no elastic displacement would have occurred.

The following estimate along similar lines

as that performed by van de Ven and Hunter (7) but accommodated to the situations in our suspensions, checks whether such a mechanism can account for the energy dissipation:

On formation and separation of a pair, spheres in the vicinity but belonging to the layers of the colliding spheres are entrained over a distance δ with respect to the immediately surrounding liquid (which was thought to be initially at rest toward the spheres, i.e., the liquid indicated by shaded areas in Fig. 12a). The Stokes friction force is then $6\pi\lambda\eta_0 vr$, where v is the velocity of the spheres toward the liquid and λ is a correction factor of order unity because the spheres are surrounded partially by liquid with a different velocity (viz. near their apices). If τ_1 is the contact time of the formed pair, $v = \delta/\tau_1$; τ_1 will be equal to $2\beta\bar{r}/D(2\bar{r} + d)$, where $2\bar{r}/D(2\bar{r} + d)$ is the total time of the passage of two spheres; β is a correction factor of order 1/2. The energy dissipated through the motion of one sphere in the vicinity of the colliding spheres then becomes

$$E_i = 6\pi\eta_0\lambda \frac{\delta^2}{\tau} r = 6\pi\eta_0\lambda\delta^2 D(2\bar{r} + d)/2\beta. \quad [7]$$

The total energy dissipated during one collision is

$$\sum_i E_i = 2 \times 6\pi\eta_0\lambda D(2\bar{r} + d)/2\beta \times \sum \delta^2 n_\delta. \quad [8]$$

Here, n_δ is the number of spheres entrained in one layer over a distance δ; the factor 2 takes account of the fact that spheres in two adjacent layers are entrained on a collision. Relation [8] becomes independent of D if $\sum \delta^2 n_\delta$ is inversely proportional to D. Thus, if δ is constant over a certain area in one layer of radius l, n_δ is the number of spheres in a layer covering an area πl^2, thus:

$$n_\delta = \pi l^2/2\bar{r}^2 3^{1/2}. \quad [9]$$

If we take for δ 6μ and for $\sum_i E_i$ in (8), 2×10^{-4} g cm^2 sec^{-2}, we obtain for $l/\bar{r}$ reasonable values: 5 at $D = 100$ sec^{-1}, 9 at $D = 30.5$ sec^{-1}. Only at still lower D values, l/r becomes impracticably large; however, in this region deviations from the Bingham behavior begin to appear. Thus, a reasonable number of entrained spheres can account for the energy dissipation.

In addition, some energy dissipation may occur by rotation of individual spheres caused by the nonzero vorticity component of simple shear flow; thus an even smaller number of entrained spheres than given by the preceding estimate can account for the energy dissipation. In the present state of our knowledge, however, no reliable estimate of this effect appears possible.

Part of the local stress caused by a collision must be caught elastically if the correct dependence on D is to be obtained (thus, the difference between the energies dissipated on an encounter at $D = 100$ sec^{-1} and at $D = 30.5$ sec^{-1} as calculated should be due to elastical storage of the energy). It might be objected that this would involve quite a large number of particles, in view of the weak bonds between the particles; however, if the layers are so densely packed that the primary particles cannot easily turn aside, compressive stresses will occur which can store a large amount of energy.

From these results we conclude that the energy dissipation corresponding with $\tau_0 \times D$ in noncoagulating suspensions in stationary flow cannot be accounted for by the energy released on pair formation and necessary for pair separation. The motion of entrained spheres in the vicinity of a colliding pair must be taken into consideration, but this can only provide an energy dissipation proportional to D if the number of entrained spheres decreases with increasing mutual velocity of the colliding spheres. A mechanism which might provide this effect is, that during a slow encounter, the local stress caused by a collision brings about viscous motion of neighboring spheres, whereas on a rapid encounter a

larger fraction of the local stress is caught elastically.

It should be noted, that this model is developed for, and in the present paper applied only to the flow of noncoagulated suspensions in the c_v region between 0.4 and 0.6.

CONCLUSIONS

Making the surface of glass particles hydrophobic effects coagulation in glycerol + water mixtures, but no effect is seen in dioctyl phthalate. Suspensions of glass particles in DOP are therefore considered to be noncoagulating. The energy dissipation in stationary flow in these suspensions cannot be connected with the energy released on pair formation and necessary for pair separation.

APPENDIX 1: *Calculation of the chance that a passage of two spheres in adjacent layers leads to a collision on the basis of deviations from the average radius (K_1)*

A particular sphere, called "central" for shortness' sake and designated below by the suffix 1, will come into contact with a sphere in the neighboring layer if

$$r_1 + r_2 \geq ((2\bar{r} + d)^2 + y_2^2)^{1/2} \quad [A1]$$

(see Fig. 15). Thus, if $r_1 = \bar{r} + u_1$ and $r_2 = \bar{r} + u_2$, the central sphere will contact any sphere in the neighboring layer for which

$$u_2 \geq ((2\bar{r} + d)^2 + y_2^2)^{1/2} - 2\bar{r} - u_1 \equiv u_{\text{lim}}. \quad [A2]$$

Thus, a central sphere with a certain u_1 value will have, on passing a neighbor, a collision chance equal to

$$\frac{\int_{y_2=-2r}^{+2r}\int_{u_2=u_{\text{lim}}}^{3\sigma} \exp(-(u_2^2/2\sigma^2))du_2dy_2}{\int_{y_2=-2r}^{+2r}\int_{u_2=-3\sigma}^{+3\sigma} \exp(-(u_2^2/2\sigma^2))du_2dy_2}, \quad [A3]$$

where σ is the standard deviation of the radius, $=(1/2)\sigma_\phi$. The integration limits for u_2 are taken at -3σ and $+3\sigma$ in order to avoid negative radii. The chance that an arbitrary passage will lead to a collision will then be given by

$$K_1 = \frac{\int_{u_1=-3\sigma}^{+3\sigma}\int_{y_2=-2r}^{+2r}\int_{u_2=u_{\text{lim}}}^{+3\sigma} \exp(-(u_1^2 + u_2^2)/2\sigma^2)du_1du_2dy_2}{\int_{u_1=-3\sigma}^{+3\sigma}\int_{y_2=-2r}^{+2r}\int_{u_2=-3\sigma}^{+3\sigma} \exp(-(u_1^2 + u_2^2)/2\sigma^2)du_1du_2dy_2}. \quad [A4]$$

Table II shows some values calculated for K_1 (glass sample 3).

APPENDIX 2: *Calculation of the chance that two spheres, both with "average" radius, will contact during a passage because of deviations of their centers from the centers of their respective layers. (K_2)*

If h_1 and h_2 are the deviations of the two passing spheres from the centers of their respective layers, the two spheres will contact when

$$h_1 + h_2 + (4\bar{r}^2 - y_2^2)^{1/2} > 2\bar{r} + d. \quad [A5]$$

Thus, the collision chance for a sphere with a certain h_1 value during a passage is

$$\frac{\int_{y_2=-2r}^{+2r}\int_{h_2=h_{\text{lim}}}^{r3^{1/2}} f(h_2)dh_2dy_2}{\int_{y_2=-2r}^{+2r}\int_{h_2=-r3^{1/2}}^{r3^{1/2}} f(h_2)dh_2dy_2} \quad [A6]$$

with

$$h_{\text{lim}} = 2\bar{r} + d - (4r^2 - y_2^2)^{1/2} - h_1. \quad [A7]$$

$f(h_2)$, the probability of finding a sphere on a distance h_2 from the center of its layer,

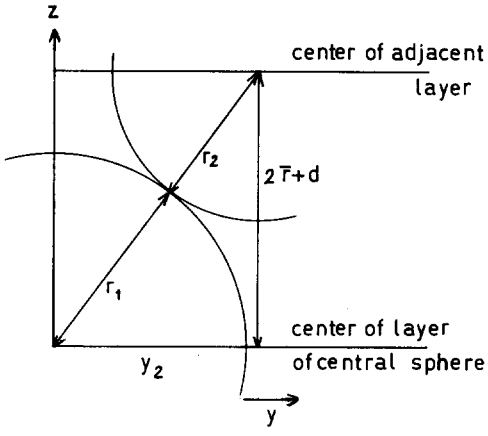

FIG. 15. Conditions leading to a collision between spheres with centers in the centers of their respective layers but with radii deviating from $\bar{r}$. Seen in the direction of motion (= the x axis).

is thought to be determined by the quotient of the additional frictional energy, spent by the liquid medium between the layers because of h_2 being $\neq 0$, to the fraction of the viscous energy dissipation between the layers which is used for disarranging the layers. The former is estimated to be

$$E_{\text{extra}} = 3\pi\eta_0 D^2\left(\frac{2r+d}{d}\right)^2 |h_2|^3 \quad [A8]$$

on the basis of the following reasoning: that part of the surface of sphere A in Fig. 16, which is situated between h_2' and $h_2' + dh_2$, is surrounded by a liquid with relative velocity $v = D \times ((2r + d)/d) \times h_2'$. The frictional force experienced by this part of the surfaces $= (2\pi r dh'/4\pi r^2) \times 6\pi\eta_0 rv$, and the energy dissipated per unit of time becomes

force $\times$ velocity

$$= 3\pi\eta_0 D^2\left(\frac{2r+d}{d}\right)^2 h'^2 dh'. \quad [A9]$$

After integration between the limits $h' = 0$ and h_2 we obtain relation [A8]. Here the absolute value of h_2 is used because a negative value of h_2 means that the sphere concerned will protrude beyond its neighbors at the lower side of its layer.

In the foregoing, the liquid between the layers was assumed to experience laminar motion. Though this may give an indication of the average force experienced by a sphere protruding from its surroundings, it is of course a simplification. Part of the viscous forces exerted on the spheres will disarrange the layers rather than form them. We assume that a certain fraction of the energy dissipated by the liquid between the layers is spent for disarranging the layers.

The total viscous energy dissipated per second in the liquid between two adjacent layers is $\tau \times D_1 \times A \times d$ for a surface area A of the adjacent layers. Here D_1 is the local velocity gradient in the liquid film, $=D((2r + d)/d)$. We estimate the part of this energy used for disarranging one particular sphere in the layers, by considering that this sphere is surrounded by moving liquid on two sides; in both adjoining liquid films a volume $2r^2 3^{1/2} \times (1/2)d$ can be assigned to the sphere concerned; the total energy dissipated per second in this volume is

$$\tau \times D_1 \times 2r^2 3^{1/2} \times d = \eta_0 \times D_1^2 \times 2r^2 3^{1/2} \times d. \quad [A10]$$

Of this dissipated energy, only part will be disarranging the sphere concerned; this we take into account by assigning an effective area $A < 2r^2 3^{1/2}$ to the sphere which is used

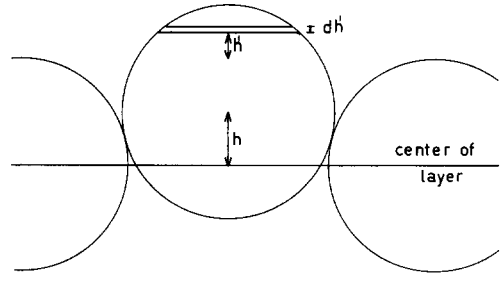

FIG. 16. Figure illustrating the parameters h' and dh' for a sphere whose center deviates a distance h from the center of its layer.

as a parameter. By combining [A8], [A9], and [A10] we obtain

$$f(h_2) = K \times \exp(-\pi |h_2|^3/(A \times d), \quad [A11]$$

where K is a constant, determined by the normalization condition

$$\int_{h_2=-r3^{1/2}}^{+r3^{1/2}} f(h_2)dh_2 = 1. \quad [A12]$$

Thus we obtain, by inserting relation [A11] into [A6] and taking into account the probability that sphere 1 will have a deviation h_1 from the center of its layer:

$$K_2 = \frac{\int_{h_1=-r3^{1/2}}^{+r3^{1/2}} \int_{y_2=-2r}^{+2r} \int_{h_2=h_{\lim}}^{+r3^{1/2}} \exp(-(\pi(|h_1|^3 + |h_2|^3)/A \times d))dh_1dh_2dy_2}{\int_{h_1=-r3^{1/2}}^{+r3^{1/2}} \int_{y_2=-2r}^{+2r} \int_{h_2=-r3^{1/2}}^{+r3^{1/2}} \exp(-(\pi(|h_1|^3 + |h_2|^3)/A \times d))dh_1dh_2dy_2}. \quad [A13]$$

Table II shows some values calculated for K_2 (glass sample 3).

APPENDIX 3: NOMENCLATURE

A = effective area for transmitting the energy of interlayer viscous flow for disarranging a sphere from its layer.
A_{12} = Hamaker constant ($g \cdot cm^2 \cdot sec^{-2}$)
a = floc radius
c_v = solid volume fraction
D = velocity gradient (sec^{-1})
d = average thickness of space between the layers formed by suspended spheres in flow
E_i = energy dissipated through the motion of sphere i in the vicinity of a colliding pair
E_L = energy dissipated per unit of volume and time in stationary flow, by momentum transfer between flow units of the suspending medium
E_{SL} = energy dissipated per unit of volume and time by interaction between the suspended particles and the suspending medium
H = distance of closest approach between two colliding spheres
h = deviation of a center of a sphere from the center of its layer
K_1 = chance that the passage of two spheres in adjacent layers, with their centers in the centers of their respective layers, but with radii deviating from the average, is accompanied by a collision
K_2 = chance that the passage of two spheres in adjacent layers, both with average radius but with centers deviating from the centers of their respective layers, is accompanied by a collision
K_3 = overall chance that a collision occurs on passage of two spheres in adjacent layers
l = radius of area in one layer where spheres are entrained during a collision
M = torque exerted on inner cylinder ($g \cdot cm^2 \cdot sec^{-2}$)
N_0 = number of particles per unit volume
n_δ = number of spheres entrained over a distance δ by a colliding sphere in their vicinity
p = number of particles colliding with one particle per unit of time
R_{ij} = collision radius
r = radius of spherical suspended particle (μm)
$\bar{r}$ = average value of radius of spherical suspended particle, chosen such as to make 50% by volume of the glass sample smaller than $(4/3)\pi\bar{r}^3$ (μm)
u = deviation of the radius of a sphere from $\bar{r}$

u_{lim} = value of u for which two passing spheres just touch

v = velocity of a sphere toward the surrounding liquid

y = coordinate in the direction perpendicular to both the direction of motion and the direction of the velocity gradient

α_0 = capture efficiency, i.e., the probability that an encounter between two suspended particles leads to pair formation

β = correction factor (of order 1/2), for calculating the contact time between two passing spheres from the time needed for a passage

δ = distance travelled by spheres entrained by a colliding sphere in their vicinity

η = viscosity (for Newtonian liquid); plastic viscosity (for Bingham liquid)

η_0 = viscosity of suspending medium

λ = correction factor (of order unity) for Stokes friction force

σ = standard deviation of radius (μm)

σ_ϕ = standard deviation of volume fraction vs ϕ distribution (μm)

τ = shearing stress ($g \cdot cm^{-1} \cdot sec^{-2}$)

τ_0 = Bingham yield value ($g \cdot cm^{-1} \cdot sec^{-2}$)

τ_1 = contact time of a pair of colliding spheres

ϕ = diameter of glass spheres (μm)

REFERENCES

1. Smoluchowski, M. V., *Z. Phys. Chem.* **92,** 129 (1917).
2. Overbeek, J. Th. G., *in* "Colloid Science" (H. R. Kruyt, Ed.), Vol. I, p. 324. Elsevier, Amsterdam, 1952.
3. van de Ven, T. G. M., and Mason, S. G., *Colloid Polym. Sci.* **255,** 468 (1977).
4. Firth, B. A., and Hunter, R. J., *J. Colloid Interface Sci.* **57,** 248 (1976).
5. Firth, B. A., *J. Colloid Interface Sci.* **57,** 257 (1976).
6. Firth, B. A., and Hunter, R. J., *J. Colloid Interface Sci.* **57,** 266 (1976).
7. van de Ven, T. G. M., and Hunter, R. J., *Rheol. Acta* **16,** 534 (1977).
8. Hunter, R. J., and Frayne, J., *J. Colloid Interface Sci.* **76,** 107 (1980).
9. Kao, S. V., Nielsen, L. E., and Hill, C. T., *J. Colloid Interface Sci.* **53,** 358 (1975).
10. Kao, S. V., Nielsen, L. E., and Hill, C. T., *J. Colloid Interface Sci.* **53,** 367 (1975).
11. Hoffman, R. L., *Trans. Soc. Rheol.* **16**(1), 155 (1972).
12. Hoffman, R. L., *J. Colloid Interface Sci.* **46**(3), 491 (1974).
13. Overbeek, J. Th. G., *in* "Colloid Science" (H. R. Kruyt, Ed.), Vol. I, p. 270. Elsevier, Amsterdam, 1952.
14. McGown, D. N. L., and Parfitt, G. D., *Discuss. Faraday Soc.* **42,** 225 (1965).
15. Friend, J. P., and Hunter, R. J., *J. Colloid Interface Sci.* **37,** 548 (1971).